Modeling and Analysis of the X-ray Powder Diffraction Structure of γ-Zirconium Phosphates Pillared with Butyl Chains through Molecular Dynamics Simulations

Giulio Alberti,[†] Giuseppe M. Lombardo,[‡] Giuseppe C. Pappalardo,*[,‡] and Riccardo Vivani[†]

Dipartimento di Chimica, Università di Perugia, via Elce di Sotto 8, 06123 Perugia, Italy, and Dipartimento di Scienze Chimiche, Cattedra di Chimica Generale, Facoltà di Farmacia, Università di Catania, Viale A. Doria 6, 95125 Catania, Italy

Received June 25, 2001. Revised Manuscript Received September 20, 2001

Detailed insights into the structural features of γ-zirconium phosphate pillared with butyl chains were obtained by molecular dynamics simulations (NPT and NVT type) of models. The available X-ray powder diffraction structure provided reasonable initial conditions (interlayer distances and unit cell parameters) to generate the models submitted to the simulations (timing 1 ns). Using the results of the molecular dynamics trajectories, the X-ray structure of the compound was adequately reproduced by an average of the structural models corresponding to the four accessible orientations of the butyl chains toward the *a* and *b* cell axes. This result showed that, in the crystallite, the chains were arranged along the four possible orientations. The predominant structural motif of the molecular assembly in the bulk of pillared γ-zirconium phosphate butyldiphosphonate was found to be composed of layers laid one upon the other with the pillars of each layer pointing in the same direction, with rare interruptions of this sequence by opposite positioning of the butyl chains of two interfaced layers. The molecular dynamics technique was thus found to be a valid approach to solving otherwise intractable issues concerning structural features of γ-zirconium phosphate derivatives pillared with aliphatic chains, and it is likely that this promising technique can be extended to a variety of similar compounds.

Introduction

Since the preparation of the first zirconium phosphonates by one of the authors,[1] the chemistry of lamellar metal phosphonates has been intensively investigated in many laboratories, and comprehensive surveys are now available.[2,3] The formation of derivative compounds of α- and γ-zirconium phosphates (herewith α-ZrP and γ-ZrP, respectively) in which the adjacent layers are covalently pillared by rigid organic or inorganic moieties has also been reported.[4,5] The pillared compounds are of interest in the fields of tailor-made molecular sieves,[6,7] shape-selective catalysis,[8] and layer-by-layer growth of ultrathin films with oriented pillars.[9]

Recently, compounds able to give an "accordion-like movement" have been prepared by pillaring γ-zirconium phosphate with nonrigid pillars such as 1,*n*-alkanediphosphonate chains.[10] These materials are a unique class of highly tailorable molecules, because their properties can be modulated through changes in the number of the carbon atoms of the alkyl chain, the degree of pillaring, and the amount of solvent included in the interpillar spaces.

Although the first pillared γ-zirconium phosphonates were obtained in 1993,[11] the present structural information on these materials is still poor, thus hindering or preventing new developments.

The major impediment to understanding the structural and conformational features of pillared γ-ZrPs is that they are obtained only as powders, often of low crystallinity or amorphous form, thus making structure determinations by X-ray analysis difficult or impossible. The structural information that can be obtained from X-ray powder diffraction (XRPD) decreases with increasing length of the alkyl chain.

The force field (FF) technique is a powerful computational tool for investigating large polyatomic molec-

* To whom address correspondence. E-mail: gcpappalardo@dipchi.unict.it.
[†] Università di Perugia.
[‡] Università di Catania.

(1) Alberti, G.; Costantino, U.; Allulli, S.; Tomassini, N. *J. Inorg. Nucl. Chem.* **1978**, *40*, 1113.
(2) Alberti, G. Layered Metal Phosphonates and Covalently Pillared Diphosphonates. In *Comprehensive Supramolecular Chemistry*; Alberti G., Bein, T., Eds.; Pergamon Press and Elsevier Science Ltd.: Oxford, U.K., 1996; Vol. 7, p 151.
(3) Clearfield, A. In *Progress in Inorganic Chemistry*; Karlin, K. D., Ed.; John Wiley & Sons: New York, 1998; Vol. 47, p 374.
(4) Alberti, G.; Costantino, U.; Vivani, R.; Zappelli, P. *Angew. Chem., Int. Ed. Engl.* **1993**, *32*, 1357.
(5) Alberti, G.; Marmottini, F.; Murcia-Mascarós, S.; Vivani, R. *Angew. Chem., Int. Ed. Engl.* **1994**, *33*, 1594.
(6) Alberti, G.; Vivani, R.; Marmottini, F.; Zappelli, P. *J. Porous Mater.* **1998**, *5*, 205.
(7) Alberti, G.; Casciola, M.; Costantino, U.; Vivani, R. *Adv. Mater.* **1996**, *8*, 291.
(8) Dines, M. B.; Di Giacomo, P. M. *Inorg. Chem.* **1981**, *20*, 92.
(9) Yang, H. C.; Aoki, K.; Hong, H. G.; Sackett, D. D.; Arrendt, M. F.; Yau, S. L.; Bell, C. M.; Mallouk, T. E. *J. Am. Chem. Soc.* **1993**, *115*, 11855.
(10) Alberti, G.; Murcia-Mascarós, S.; Vivani, R. *J. Am. Chem. Soc.* **1998**, *120*, 9291.
(11) Alberti, G.; Murcia-Mascarós, S.; Vivani, R. *Mater. Chem. Phys.* **1993**, *35*, 187.

10.1021/cm011156g CCC: $22.00
Published on Web 12/05/2001

ular systems. In a previous work, we showed that the FF approach implemented with ad hoc quantum mechanically derived parameters is suited to the study of the structures of layered zirconium phosphates.[12] The application of FF calculations can thus be extended to these systems even when modified by pillaring. The XRPD spectra of γ-ZrPs pillared with nonrigid alkyl chains show wide overlapping bands, thus providing incomplete structural information. The availability of a suitable FF allows these systems to be studied using molecular dynamics (MD) simulations. Within the framework of the MD scheme it is possible to (i) monitor internal molecular fluctuations, (ii) generate microscopic-level information that can be correlated directly with experimentally detectable macroscopic properties, (iii) support the refinement and interpretation of X-ray diffraction data of low-crystallinity solids, and (iv) validate models of the real system by comparison with experimental data. Among the main advantages provided by MD simulations of lamellar materials is the possibility of revealing structural, conformational, and functional properties that are directly inaccessible by experimental methods. In this work, we focused on the layered and pillared γ-zirconium phosphate butyldiphosphonate dihydrate, γ-$ZrPO_4[O_2P(OH)C_4H_8(OH)PO_2]_{0.5}\cdot 2H_2O$ (hereafter γ-ZrPB), using MD simulations to interpret the XRPD structure.[13] The goal of this paper is two-fold: first to provide additional experimental information about the structure and conformation of γ-ZrPB and its molecular assembly in the bulk (solid state), i.e., its three-dimensional molecular order, and second, to extend the use of computational chemistry for the analysis of XRPD structural data for describing the three-dimensional arrangement, molecular assembly, and conformational and functional features of pillared γ-ZrP materials that are short-range-ordered or amorphous in nature and are not amenable to single-crystal X-ray diffraction.

MD Simulations

Protocols. The Cerius[2] package developed by BIOSYM/MSI was used to perform all MD calculations through the OFF (open force field) routine that includes the empirical functions of the universal FF. The crystal facility of this program was used for reproducing the periodic boundary conditions (PBC), which are needed to avoid border effects.

The FF techniques for lamellar systems require a suitable set of parameters for all of the internal coordinates of the uncommon structural units in these materials. The universal FF parameters derived by us for zirconium phosphates[12] were used in this work. To derive the additional FF parameters needed for γ-ZrPB, we used the technique of energy derivatives obtained from ab initio quantum mechanics on a model compound as outlined by Dinur and Hagler.[14] The whole set of parameters used is quoted in Table 1.

The atomic charges were obtained with the charge equilibration method[15] implemented in the Cerius[2] package. All of the simulations were started from energy-minimized structures obtained through the conjugate gradient method, satisfying a gradient of ≤ 0.1 kJ mol^{-1} Å^{-1}. The evolutions were carried out using either the NPT (constant pressure and temperature) or the NVT (constant volume and temperature) algorithm and the Nosé thermostat.[16] The temperature and external pressure (where it applies) were set at 298 K and 0.0 GPa, respectively, with a thermal bath coupling constant of 0.1 ps and a cell mass prefactor of 1.0.

The scale factor for the nonbond (NB) 1−4 interactions was set to 0.5. The NB interaction cutoff was implemented using the Ewald procedure of lattice sums.[17] The dielectric constant (ϵ) was set to 1. Transients for 1 ns with a sampling interval of 0.2 ps were usually collected. The integration time step was 0.001 ps.

For simulating models **6A** and **6B**, we used a distance-dependent dielectric constant and the SPLINE cut off method for the nonbonded interactions (with spline-on distance = 20.0 and spline-off distance = 25.0 Å) to mimic the solvent.

Models. Based on the symmetry data provided by XRPD[13] (orthorhombic cell, $a = 5.3797(2)$, $b = 6.6244(2)$, $c = 13.0111(5)$ Å, space group *Pmmn*), four structural models of type 1 γ-ZrPB were first considered, corresponding to the accessible orientations of the butyl chain toward the *a* and *b* cell axes. By assuming the origin of the axes at the P2 atom, the four

Table 1. Universal Force Field (UFF) Set of Parameters for γ-ZrPB[a]

parameter	l_0 (Å)	k_s (kcal mol^{-1} Å^{-2})
Zr−O	2.0646	171.66
P−O	1.5300	1096.36
P−C(P)	1.8252	394.70
C(P)−C	1.5820	311.76
C(P)−H	1.1061	666.13

parameter	α_0 (°)	k_b (kcal mol^{-1} deg^{-2})	l_0 (Å)	k_{UB} (kcal mol^{-1} Å^{-2})
O−Zr−O	90.00	149.23	2.920	128.60
(O−Zr−O)	180.00	8.74	4.130	90.90
Zr−O−P	150.81	169.45	3.460	251.34
O−P−O	109.47	140.24	2.500	96.07
P−O−H	112.82	104.92	2.000	81.68
H−C(P)−H	107.94	91.42	1.782	14.89
C−C(P)−H	112.00	115.00	2.266	6.70
P−C(P)−H	108.02	145.43	2.405	5.78
P−C(P)−C	109.01	141.64	2.776	74.01

parameter	k_ϕ (kcal mol^{-1})	n	ϕ_0
Zr−O−P−O	20.930	1	0.0
	0.750	2	0.0
	0.116	3	0.0
O−Zr−O−P	9.732	1	0.0
	2.836	2	0.0
	0.790	3	0.0
(O−Zr−O)−P	0.0[b]	1	0.0
O−P−O−H	12.920	1	0.0
	3.210	2	0.0
	0.008	3	0.0
O−P−C(P)−C	15.815	1	0.0
	6.444	2	0.0
	0.917	3	0.0
Zr−O−P−C(P)	22.593	1	180.0
	4.564	2	180.0
	0.217	3	180.0
O−P−C(P)−H	6.529	1	180.0
	0.808	2	0.0
	0.175	3	180.0

[a] Default values of the UFF are valid for the remaining parameters not quoted in the table. [b] Torsional angle (O−Zr−O)−P is neglected because of the (O−Zr−O) bond angle of 180°.

(12) Alberti, G.; Grassi, A.; Lombardo, G. M.; Pappalardo, G. C.; Vivani, R. *Inorg. Chem.* **1999**, *38*, 4249.
(13) Alberti, G.; Vivani, R.; Murcia Mascarós, S. *J. Mol. Struct.* **1998**, *469*, 81.
(14) Dinur, U.; Hagler, A. T. In *Reviews in Computational Chemistry*; Lipkowitz, K. B., Boyd, D. B., Ed.; VCH Publishers: New York, 1991; Vol. 2, p 99.
(15) Rappe A. K.; Goddard, W. A., III. *J. Phys. Chem.* **1991**, *95*, 3358.
(16) Nosé, S. *J. Chem. Phys.* **1984**, *91*, 511.
(17) Karasawa, N.; Goddard, W. A., III. *J. Phys. Chem.* **1989**, *93*, 7320.

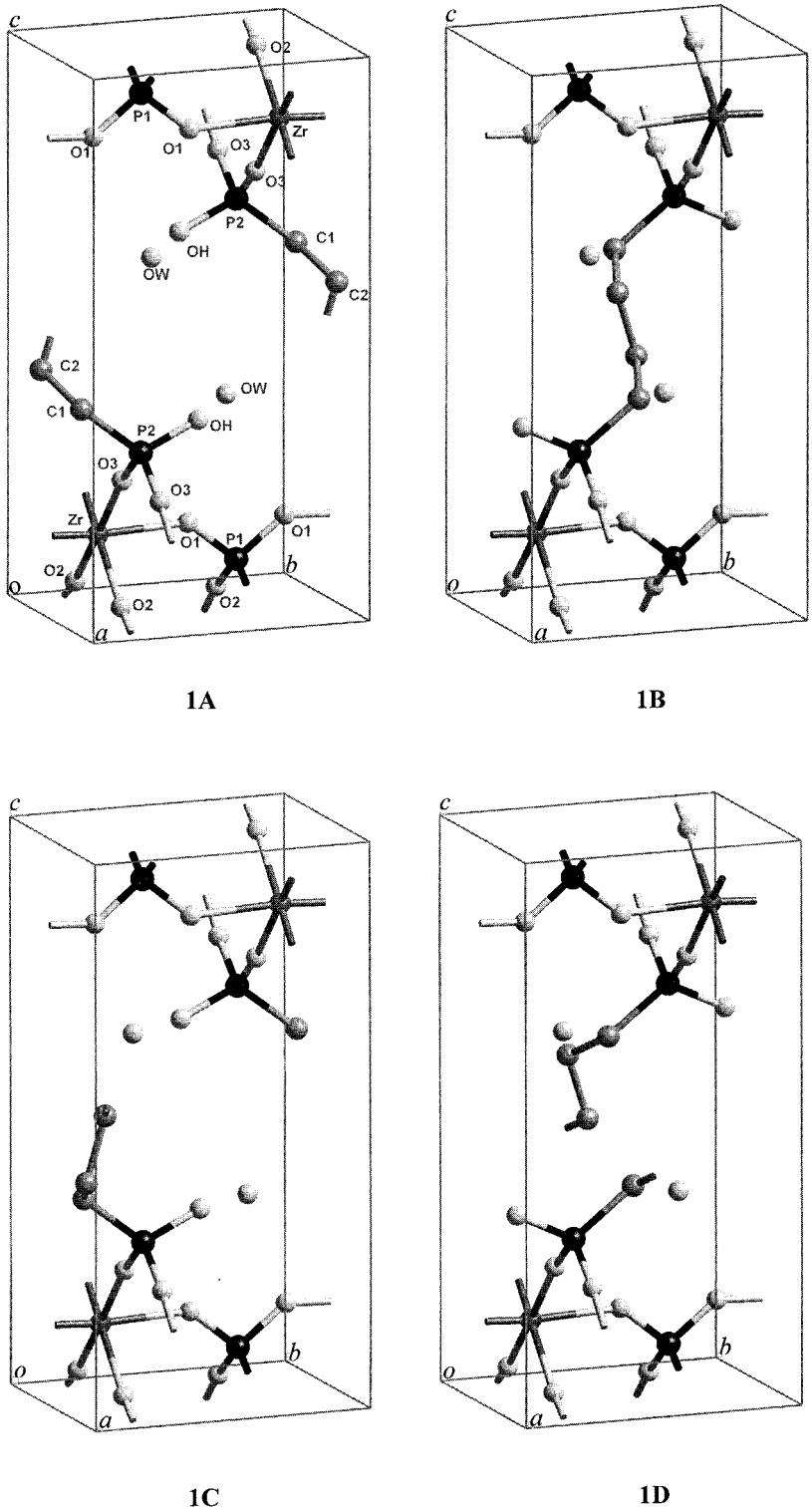

Figure 1. Perspective views of structural models **1A**−**1D** of γ-ZrPB corresponding to the accessible orientations of the butyl chain toward the *a* and *b* cell axes.

orientations of the butyl chains were denoted as **A** (−*a*, −*b*), **B** (−*a*, +*b*), **C** (+*a*, −*b*), and **D** (+*a*, +*b*). These models were coded as **1A**, **1B**, **1C**, and **1D**, respectively (Figure 1).

The type 2 models were two super-cells, each constructed by repeating the single cell along its *b* axis. The models **2A** and **2B** were thus formed by pairing **1A** with **1C**, and **1B** with **1D**, respectively (Figure 2). Such an arrangement in each type 2 model obeys the condition of opposite alignments of the two butyl chains along the *a* axis [**2A**, (+*a*, −*b*) (−*a*, −*b*); **2B**, (−*a*, +*b*) (+*a*, +*b*)].

Model **3** was generated by interfacing models **2A** and **2B** in a structure in which the pillars of a layer were oriented oppositely (+*b* and −*b*) to those of the adjacent layers (Figure 3). Modification of model **3** into model **4** (Figure 4) was attained by the addition of a layer above and below model **3**: in this arrangement, two consecutive layers having pillars aligned in the same orientations (+*a*, +*a* and −*b*, −*b*) are interfaced as model **3** (+*a* and −*b*).

Models **5A**−**5D** were constructed by doubling the corresponding models **1A**−**1D** along the *c* axis. In each model, the two interfaced layers were arranged with pillars iso-oriented (Figure 5).

Models **6A** and **6B**, built to simulate the system during the reassembly of layers after the topotactic reaction,[18] each

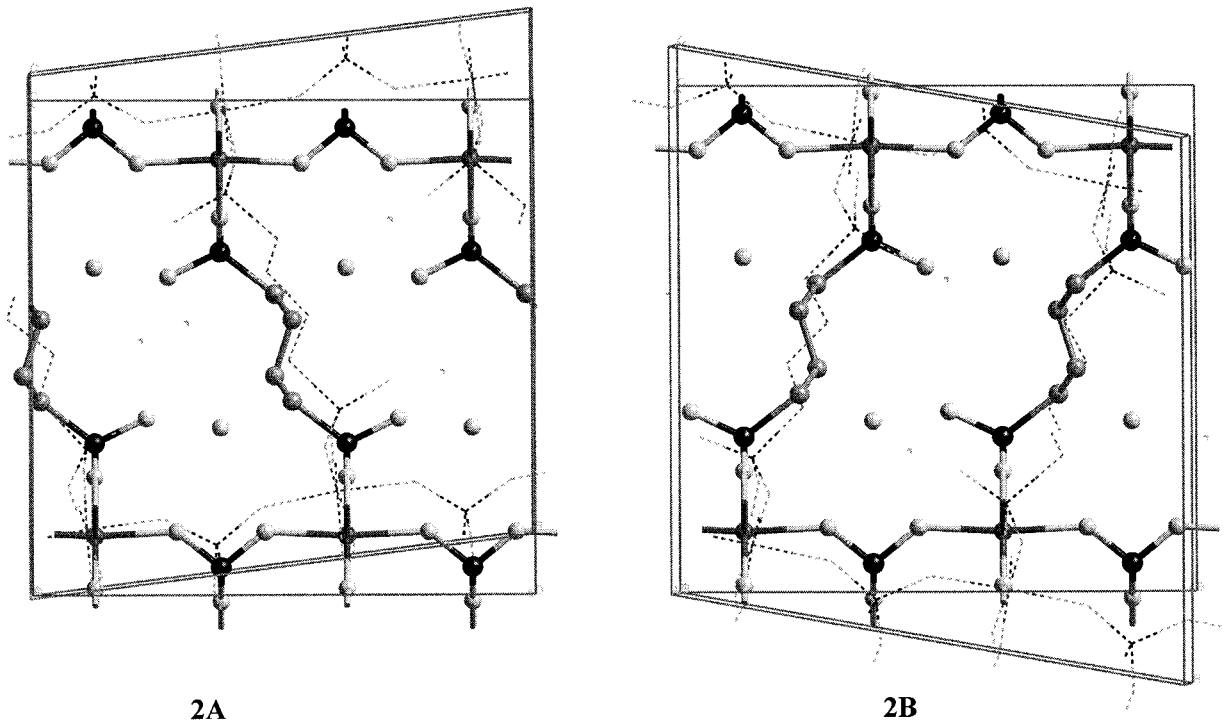

Figure 2. Models **2A** and **2B** viewed along the cell axis *a*, superimposed on a snapshot of the NPT MD trajectory (dotted line). In supercell **2A**, the directions of the chains are opposite in each supercell, that is, $+a$ and $-a$ for the chains to the left and to the right of the viewer, respectively, whereas in supercell **2B**, the directions are $-a$ and $+a$ for the chains to the left and to the right of the viewer, respectively.

contained three layers (Figure 6). They constituted a slab, with periodic conditions being imposed only on the plane of the layers (*a* and *b*). In the two interlayer spaces, the butyl chains were oriented the same [$(+a, -b)$ $(-a, -b)$, $(+a, -b)$ $(-a, -b)$] in **6A** and oppositely oriented [$(+a, -b)$ $(-a, -b)$], $(+a, +b)$ $(-a, +b)$] in **6B**. The molecular fragments protruding on the external surface of the layers were saturated with −OH groups.

Results and Discussion

In Table 2 are listed the average cell parameters obtained by NPT trajectories of models **1**−**4**. For each model, the simulations attained values for the *a* and *b* axes in good agreement with the experimental results.[13] The *c* axis was slightly overestimated for all four models (Δc from 0.128 to a maximum of 0.957). The table shows that, in the case of type 1 models, the cell angles deviated from 90°. The most significant discrepancies were found for the β angle. The deviations of β were negative, −2.7° and −21°, for models **1A** and **1B**, respectively, and positive, 13.1° and 3.9°, for **1C** and **1D**, respectively. In the case of type 2 models, the major discrepancies were concerned with α, which deviated by ca. 10° and ca. −10° in **2A** and **2B**, respectively. The β and γ angles fluctuated about the experimental value of 90°. The above differences of the cell angles depended on the alkyl chain orientations. On this basis, a more realistic model would be a model containing butyl chains equally distributed along the four possible orientations, so that the distortion effects introduced by the chains sum to zero. Accordingly, model **3** represents the smallest structural unit containing the butyl chains directed toward all four possible orientations. This model consists of two layers pillared by two pairs of chains, with the first and second pair of each pillar oriented as in models **2A** and **2B**, respectively, and thus contains two layers having oppositely oriented pillars (Figure 3). The simulation of model **3** provided average cell parameters that well reproduced the experimental data (Table 2). On the other hand, the severe mean skid (ca. 3.0 Å) of adjacent layers along the *ab* plane relative to their experimental positions caused the loss of the *Pmmn* symmetry deduced from XPRD analysis (Figure 3). The simulation of model **4** was then performed to ascertain whether a less frequent pairing in the bulk of layers having oppositely oriented pillars, as imposed in model **3,** could decrease the relative skidding between the layers. The result outlined in Figure 4 shows that the experimental cell parameters were reproduced with good approximation (Table 2) and that the relative skidding between adjacent planes significantly decreased to 0.75 Å. On the basis of the results from the entire set of NPT simulations, the chain arrangement in the crystallite was as follows: (i) the butyl chains assume the four possible orientations, (ii) adjacent layers with butyl chains all pointing in the same direction are predominant, and (iii) adjacent layers interfaced with oppositely directed butyl chains are less favored. Such a picture of the material is consistent with the XPRD structure,[13] first, because the occupancy of all four possible directions of the chains constrains the cell angles to fluctuate about the experimental value of ca. 90° and, second, because the predominant motif of layers assembled with iso-oriented chains is expected to prevent the skidding between the planes. Successive NVT simulations of models **1A**−**1D**, **5A**−**5D**, and **6A** and **6B** were performed to confirm the above-proposed structural model of γ-ZrPB.

(18) Alberti, G.; Giontella, E.; Murcia-Mascarós, S.; Vivani, R. *Inorg. Chem.* **1998**, *37*, 4672.

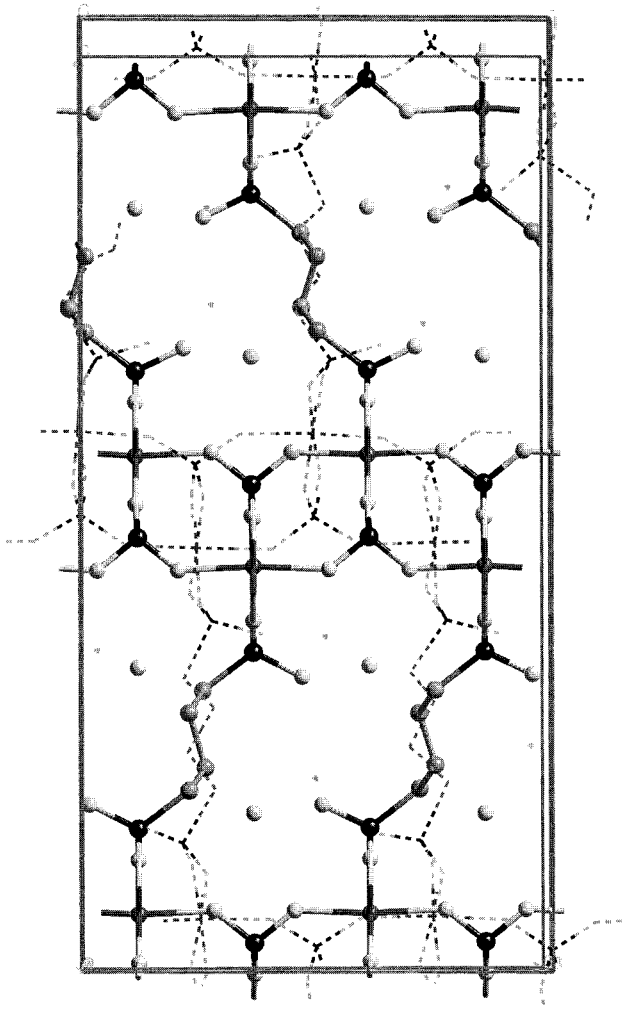

Figure 3. Model **3** viewed along cell axis *a* superimposed on a snapshot of the NPT MD trajectory (dotted lines).

The positions of the atoms of the layers in the cell obtained from the NVT trajectories of models **1A**−**1D** reproduced acceptably those from the XRPD structure (rmsd values of 0.245, 0.221, 0.230 and 0.237 for **1A**, **1B**, **1C**, and **1D**, respectively).[19] The X-ray scattering analysis reveals the average positions of the atoms in the cell, and therefore, the XRPD data must be compared with the average structure of the four models **1A**−**1D**, i.e., <**1A**−**1D**> (Figure 7). For this structure, a meaningful agreement with the experimental structure of *γ*-ZrPB was evidenced by the calculated rmsd value (0.144).

All of the type 1 models showed a significant lack of parallelism between the planes defined by O3, P2, O3′ and O3, Zr, O3′. The angle between these planes in models **1A** and **1C** and in models **1B** and **1D** was +42° and −42°, respectively.[20] This angle changed to 0° in the <**1A**−**1D**> structure, thus reproducing the experimental value. The angle between planes found for each single type 1 model is consistent with the lack of parallelism (28°) between the same set of planes determined for the parent compound *γ*-ZrP.[21] The MD NVT trajectories of models **5A**−**5D** clearly show that, because

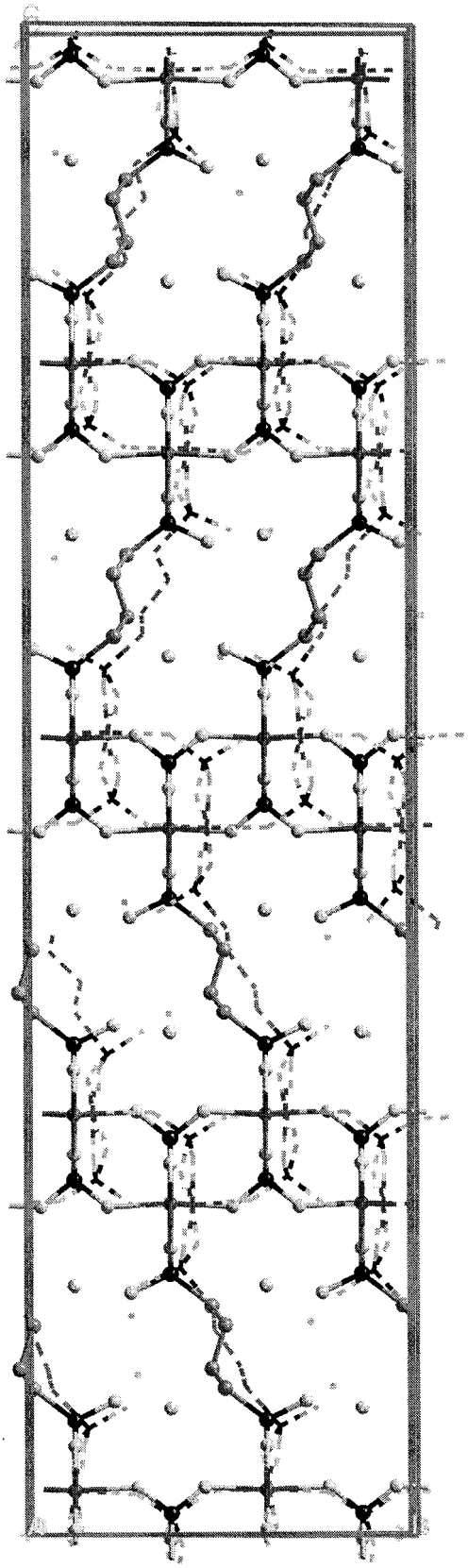

Figure 4. Model **4** viewed along cell axis *a* superimposed on a snapshot of the NPT MD trajectory (dotted lines).

(19) The rmsd values were calculated without including the C2 atom and its symmetric corresponding C2′. The cause of such an exclusion and its negligible effect will be reported and discussed in detail at the end of this section.

(20) The + and − signs were used to indicate that the P2 atoms of the models **1A**/**1C** and **1B**/**1D** were shifted towards the positive and negative directions of the *b* axis, respectively.

(21) Poojary, D. M.; Shpeizer, B.; Clearfield, A. *J. Chem. Soc., Dalton Trans.* **1995**, 111.

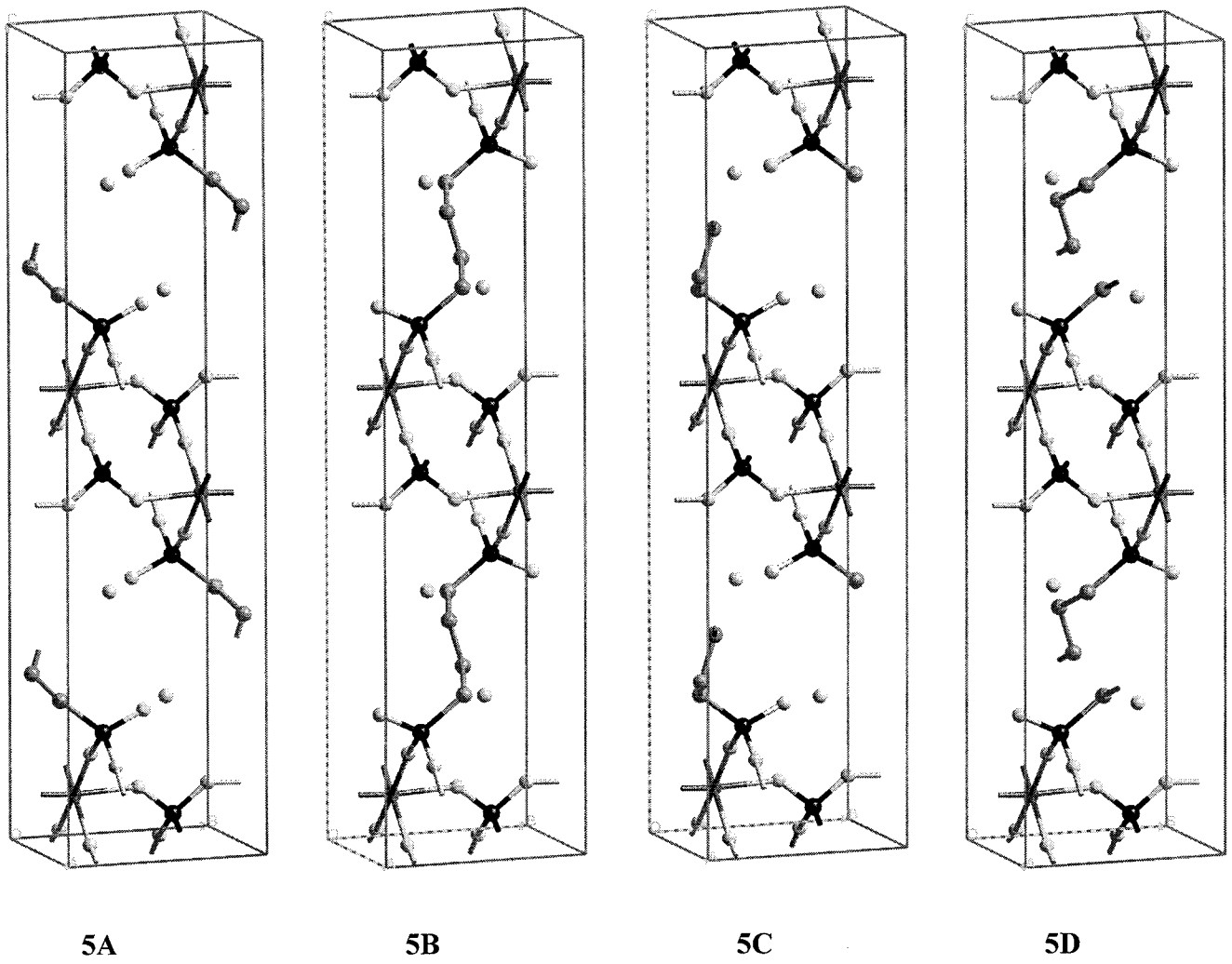

Figure 5. Perspective view of models **5A**−**5D**.

the cell angles are constrained at 90°, there is no skidding between layers with iso-oriented pillars. The average total energies calculated by the MD simulations of models **6A** and **6B** showed that **6A** is energetically favored by 8 kcal compared to **6B**. This confirmed that, after the topotactic reaction, the molecular assembly occurs along a structural motif in which the pillars of superimposed layers prefer the iso-oriented alignment (**6A**), with a small but finite probability of the inverse organization as in **6B**.

In Table 3, the bond distances and angles of the calculated structure model are compared with those of the XRPD structure of γ-ZrPB. The agreement is generally good, and some differences between the modeled <**1A**−**1D**> and XRPD structures are concerned only with selected interatomic distances (P2−OH, P2−C1, C1−C2, and C2−C2), bond angles (O1−P1−O1, O3−P2−O3, OH−P2−C1, and Zr−O2−P1), and dihedral angles (P2−C1−C2−C2, O1−Zr−O3−P2, and Zr−O3−P2−C1). The XRPD values of 102.6°, 106.1°, and 171.6°, for the O1−P1−O1, O3−P2−O3, and Zr−O2−P1 angles, respectively, are far from the values of 113.5°, 110°, and 145.8° determined for the corresponding angles in the crystal of γ-ZrP.[21] On the contrary, the bond angle values available for the γ-ZrP crystal are close to the MD-calculated values for the single-cell models of γ-ZrPB. In the case of bond distances, those featuring the XRPD structure agree with the values calculated from MD simulations of the four separate unit cells, **1A**−**1D**, but show some difference compared to the averaged <**1A**−**1D**> model. It is likely that these discrepancies are due to the Rietveld refinement of the XRPD structure that imposed the *Pmmn* symmetry group and the placement of some atoms in special crystallographic positions. The crystallite of the material contains pillar chains directed along the four possible spatial arrangements. Therefore, the atomic positions within a single structure cannot be unambiguously determined using X-ray diffraction analysis.

As to the discrepancy concerned with the torsional angle (P2−C1−C2−C2) of the butyl chains (Table 3), this cannot be safely attributed to the inherent approximation of one or both XRPD and MD techniques. However, it was verified that the conformation of the butyl moiety affects neither the interlayer distance nor the structure of the model <**1A**−**1D**> as a whole. This is because the molecular assembly and structural model depend exclusively on the relative orientation, and not on the conformation, of the pillaring butyl chains of γ-ZrPB in the bulk. Accordingly, the calculations of the rmsd values did not include the C2 and C2′ carbon atoms of the butyl chain because (i) the resulting model was unaffected by these discrepancies and (ii) during the XRPD analysis, a less accurate positioning of the

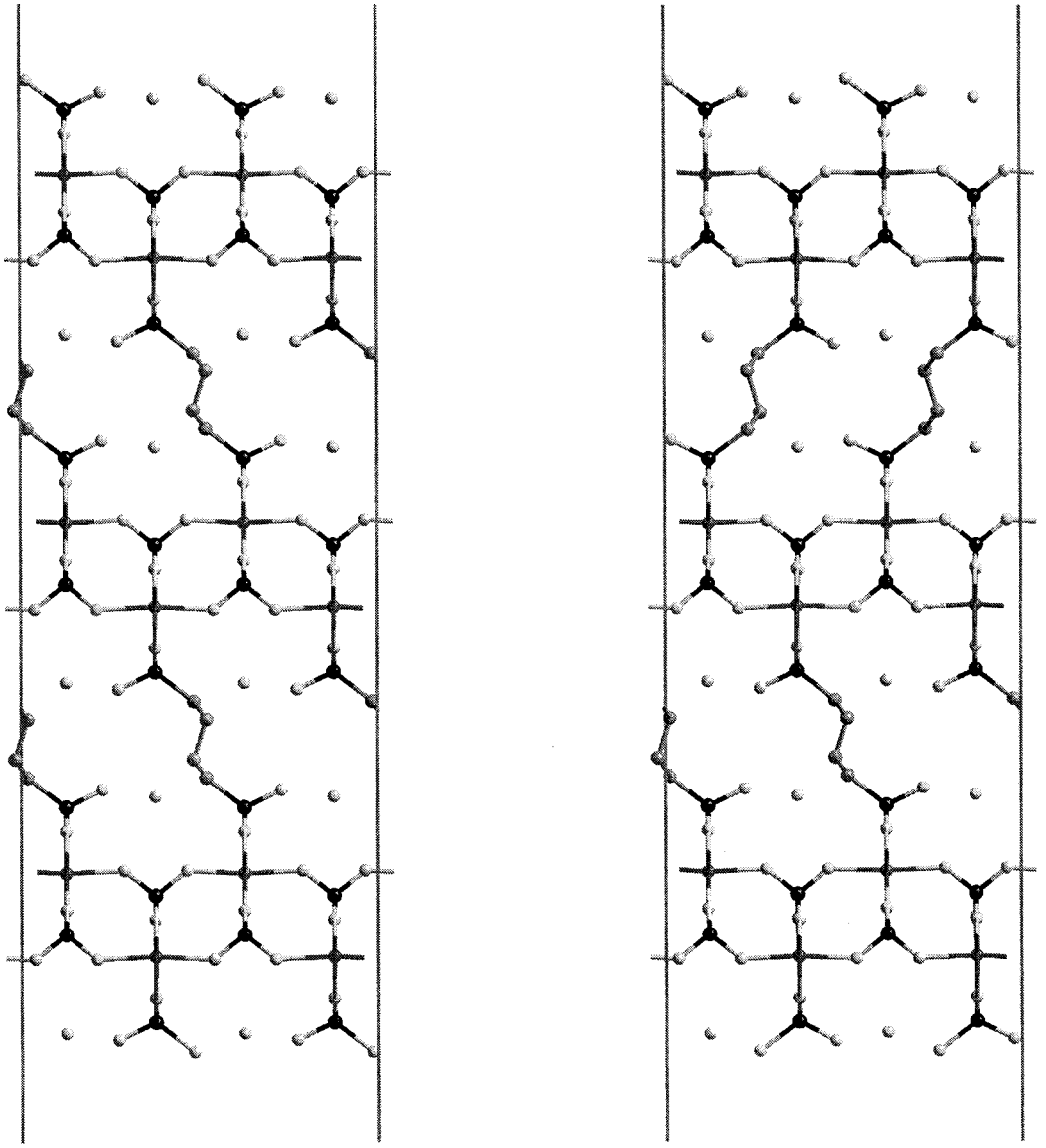

6A **6B**

Figure 6. Models **6A** and **6B** viewed perpendicularly on a plane normal to the layers.

Table 2. Average Cell Parameters for the NPT Simulations of Models 1−4 Compared with the X-ray Structure (XRPD)[a]

	1				2				
	A	**B**	**C**	**D**	**A**	**B**	**3**	**4**	XRPD
a	5.334	5.334	5.333	5.336	5.342	5.348	5.357	5.343	5.3797
b	6.663	6.666	6.666	6.666	6.684	6.666	6.674	6.675	6.6244
c	13.324	13.968	13.743	13.167	13.955	13.704	13.400	13.139	13.0111
α	88.448	89.643	87.508	91.189	80.036	97.730	90.675	90.230	90.000
β	87.316	68.837	103.154	93.860	90.071	90.696	91.317	90.016	90.000
γ	87.724	87.775	87.999	87.897	90.007	91.794	88.878	88.392	90.000

[a] Reference 11.

atoms of the butyl chain is likely as a result of critical limitations of the method when applied to the lighter carbon atoms (low resolution of the diffraction patterns, low degree of crystallinity of the samples, etc.)

Conclusions

Unique insights into the structural features of pillared *γ*-ZrPB, which were otherwise inaccessible using X-ray diffraction analysis, were achieved in this work through MD simulations of models. The structure of the material obtained from XRPD analysis was adequately reproduced by the average of the four structural models <**1A**−**1D**> corresponding to the four accessible orientations of the butyl chains toward the *a* and *b* cell axes. From the performed sets of simulations, the following still unknown features of the material were determined: (i) the four possible orientations of the pillaring butyl chains are present within the single crystallite of

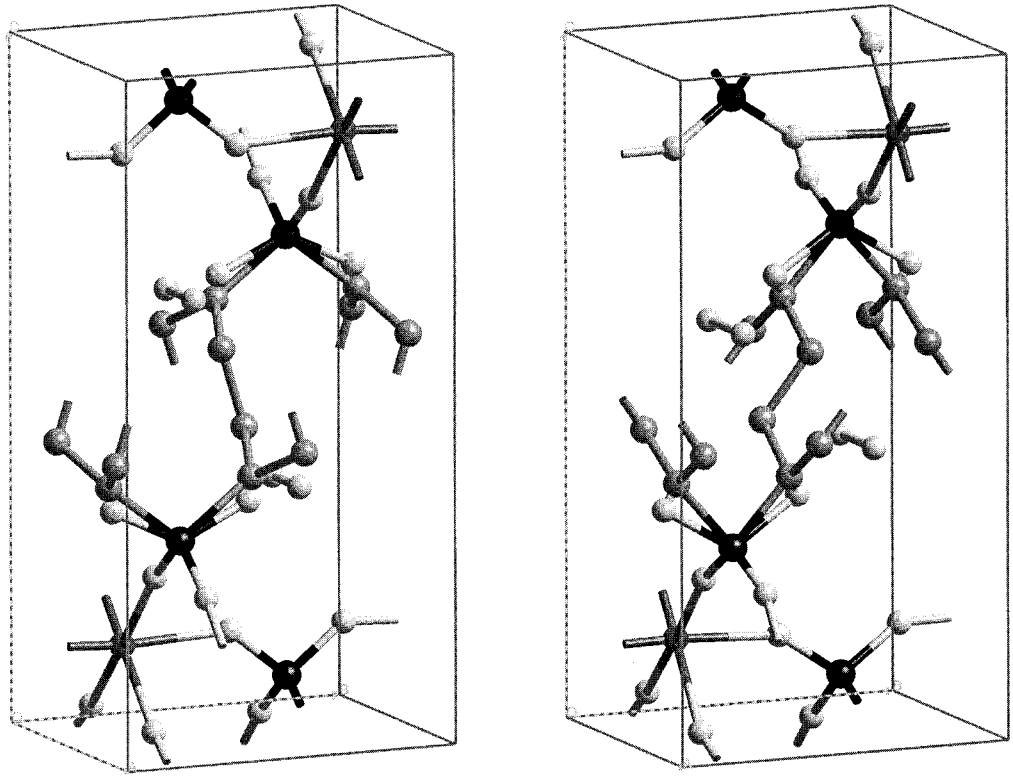

a b

Figure 7. (a) XRPD structure compared with (b) the averaged structural model <**1A**−**1D**>.

Table 3. Average Bond Lengths (Å), Angles (°), and Dihedral Angles (°) as Obtained from the NVT MD Simulations of Models of Type 1 and Averaged Structure <1A−1D> Compared with the X-ray Structure (XRPD)[a]

	A	**B**	**C**	**D**	**<1A−1D>**	XRPD
			Bond Distances (Å)			
Zr−O1	2.065	2.054	2.065	2.053	2.051	2.159
Zr−O2	2.061	2.061	2.061	2.063	2.036	1.993
Zr−O3	2.055	2.055	2.062	2.061	2.040	2.161
P2−O3	1.520	1.520	1.524	1.524	1.465	1.477
P1−O1	1.551	1.541	1.551	1.540	1.518	1.481
P1−O2	1.538	1.538	1.538	1.551	1.506	1.539
P2−OH	1.519	1.519	1.520	1.519	1.655	1.515
P2−C1	1.835	1.836	1.841	1.836	1.721	1.810
C1−C2	1.596	1.592	1.603	1.579	1.620	1.582
C2−C2	1.541	1.540	1.546	1.540	1.540	1.563
			Bond Angles (°)			
O1−Zr−O1	176.4	176.2	176.5	176.0	176.6	174.5
O1−Zr−O2	89.2	87.2	89.2	92.3	89.0	91.9
O1−Zr−O3	91.5	89.3	92.1	91.3	90.9	88.0
O2−Zr−O2	93.4	93.4	93.2	93.1	92.9	92.3
O2−Zr−O3	92.0	92.0	92.2	87.0	91.1	89.6
O2−Zr−O3	174.4	174.5	174.4	178.5	178.5	178.2
O3−Zr−O3	87.7	87.8	87.6	87.9	87.6	88.6
O1−P1−O1	112.4	112.6	112.3	112.7	112.9	102.6
O1−P1−O2	107.0	108.5	107.8	111.1	108.2	111.3
O2−P1−O2	109.5	109.4	109.4	109.2	109.1	109.0
O3−P2−O3	116.7	116.6	116.5	116.6	120.2	106.1
O3−P2−OH	116.8	116.8	117.4	115.3	103.5	105.1
O3−P2−C1	102.4	102.8	103.5	99.8	115.0	111.5
OH−P2−C1	101.3	101.0	100.6	101.7	100.4	116.7
P2−C1−C2	111.3	111.3	112.0	111.5	113.1	119.2
C1−C2−C2	111.2	111.1	111.8	112.2	110.7	107.7
Zr−O3−P2	155.9	155.8	157.1	150.6	169.3	171.3
Zr−O1−P1	142.7	146.7	142.6	146.8	148.0	148.0
Zr−O2−P1	151.5	151.4	151.4	158.3	160.9	171.6
			Dihedral Angles (°)			
Zr−O3−P2−C1	153.7	−153.2	153.0	139.0	107.6	121.7
O3−P2−C1−C2	−60.0	60.4	160.6	176.5	41.6	41.3
P2−C1−C2−C2	−169.4	170.2	167.3	−176.1	173.5	103.8
C1−C2−C2−C1	179.1	−179.6	179.9	−179.6	179.3	180.0

[a] Reference 11.

γ-ZrPB, (ii) assemblies of adjacent layers having iso-oriented pillars are the predominant motif in the bulk, and (iii) interfaces between layers having oppositely oriented pillars are disfavored.

A better knowledge of the structural features of pillared γ-ZrPB will be very important for future developments of this class of tailormade sieves and for a better interpretation of the "accordion-like movement" of the layers. On the other hand, the use of MD simulations combined with XRPD analysis appears to be a general approach for materials of low crystallinity. It is therefore reasonable to expect that the technique can also be extended to a large variety of other materials. The detailed structural information thus obtained will be very useful, in many cases, for the interpretation of experimental phenomena and for the prediction of new properties of the investigated materials.

Acknowledgment. This work was supported by MURST (PRIN 1999−2001).

CM011156G